PALAIOS
Emphasizing the impact of life on Earth's history

PALAIOS, 2009, v. 24, p. 131–136
Research Note
DOI: 10.2110/palo.2007.p07-094r

EARLY TRIASSIC MICROBIAL SPHEROIDS IN THE VIRGIN LIMESTONE MEMBER OF THE MOENKOPI FORMATION, NEVADA, USA

SARA B. PRUSS[1]* and JONATHAN L. PAYNE[2]*
[1]*Department of Geology, Smith College, Northampton, Massachusetts 01063, USA, e-mail: spruss@email.smith.edu*
[2]*Department of Geological and Environmental Sciences, Stanford University, 450 Serra Mall, Bldg 320, Stanford, California 94022; e-mail: jlpayne@stanford.edu*

ABSTRACT

Lower Triassic carbonate sedimentary rocks exhibit fabrics and facies indicative of reduced bioturbation and reduced abundance of skeletal animals and algae relative to their Permian counterparts. Widespread microbial mounds are one widely cited example. Micritic spheroids of probable microbial origin occur at a few horizons in the Spathian (uppermost Lower Triassic) Virgin Limestone Member of the Moenkopi Formation, exposed in southern Nevada. These spheroids (3–12 mm) consist of an irregular framework of micrite clots up to 100 μm in diameter and micrite-walled filaments ~10 μm wide and <500 μm long. Based upon their microstructure, we suggest that these microbial spheroids formed through the rapid microbial precipitation of calcium carbonate from seawater. As such, they probably represent unattached analogues of Early Triassic microbial mounds. The microbial spheroids formed and lithified rapidly in shallow-water, high-energy settings. Their presence, in concert with other carbonate microbialites from the Moenkopi, is consistent with the observation that microbially mediated precipitation was an important carbonate depositional mode in the aftermath of the end-Permian mass extinction.

INTRODUCTION

The end-Permian extinction, the most severe Phanerozoic mass extinction (Raup, 1979; Raup and Sepkoski, 1982), altered not only the ecological structure of marine communities (Bambach et al., 2002; McGhee et al., 2004), but also global patterns of carbonate sedimentation (Pruss et al., 2006; Baud et al., 2007). Skeletal carbonates, common in the Permian, were largely replaced by microbial carbonates (Schubert and Bottjer, 1992; Baud et al., 1997; Lehrmann, 1999; Pruss and Bottjer, 2004b), seafloor-precipitated carbonate crystal fans (Woods et al., 1999; Baud et al., 2005), and other nonskeletal sediments such as ooids (Groves and Calner, 2004; Baud et al., 2007) and micrite (i.e., carbonate mud) (Payne et al., 2006). The proportional abundances of flat-pebble conglomerate and thinly bedded carbonate mudstone, facies that typified the weakly or unbioturbated carbonate sediments deposited during the Neoproterozoic–early Paleozoic, are greater in Lower Triassic strata than in underlying or overlying units (e.g., Wignall and Twitchett, 1999; Lehrmann et al., 2001; Pruss et al., 2005b, 2006; Baud et al., 2007). Increased preservation of microbial structures and textures characterizes much of the Lower Triassic shallow marine record, suggesting reduced grazing and infaunalization of benthic invertebrates (Pruss and Bottjer, 2004a) and a reduced role for skeletal production as a calcium carbonate sink in the oceans (Baud et al., 1997; Groves and Calner, 2004; Payne et al., 2006). Thus, the sedimentary rock record and, in particular, the carbonate rock record provide evidence of changes in the Earth's system in the aftermath of severe disturbance, which is complementary to biodiversity and biogeochemical data.

The purpose of this contribution is to report the occurrence of well-preserved micritic spheroids, up to 12 mm in diameter, that are interpreted as microbial spheroids formed in shallow subtidal settings and preserved in the Virgin Limestone Member of the Moenkopi Formation in Nevada. These micritic spheroids lack the distinct layering typical of oncoids, but they appear to have formed via microbial accretion rather than micritization of bioclasts or excretion of fecal pellets. They are much larger and more regularly spherical than typical peloids. The absence of nuclei and laminations in all spheroids observed in outcrop or in thin sections suggests that the term *spheroid* may be more appropriate than the term *oncoid,* so we adopt the former term here. The internal fabric of the spheroids is similar to fabrics preserved in Early Triassic microbial mounds (Sano and Nakashima, 1997; Lehrmann, 1999; Kershaw et al., 2002; Ezaki et al., 2003; Lehrmann et al., 2003). The occurrence of spheroids in Lower Triassic carbonates further demonstrates that microbial precipitation of carbonates was not limited to microbial mounds and likely occurred in many shallow-water paleoenvironments.

GEOLOGICAL SETTING AND PALEOENVIRONMENTS

In Early Triassic time, the western United States was covered by a shallow epicontinental seaway that extended eastward to Utah and Wyoming. The Moenkopi Formation was deposited during the middle–late Early Triassic (Olenekian stage). The Virgin Limestone Member reflects deposition during the last marine incursion and is overlain in some areas by the evaporitic Schnabkaib Formation (Shorb, 1983). The Virgin Limestone Member is a mixed carbonate-siliciclastic succession that varies in thickness regionally from 50 to 300 m (Poborski, 1953; Shorb, 1983), and is ~170 m at Lost Cabin Springs (Fig. 1A). Spheroids occur at both the Lost Cabin Springs and Mountain Pass localities, where the Virgin Limestone was deposited in subtidal to peritidal paleoenvironments (Pruss et al., 2005b) (Fig. 1B).

At the Lost Cabin Springs locality, located about 60 km west of Las Vegas, the Virgin Limestone was deposited during transgression and highstand. Based on comparison with nearby localities, it appears the base of the Virgin Limestone is not exposed at Lost Cabin Springs (e.g., Pruss et al., 2005b). The lowest exposed beds of the Virgin Limestone Member at this locality consist largely of siliciclastic sediments; carbonate beds become more common higher in the exposed section. Carbonate facies at Lost Cabin Springs consist of thinly bedded carbonate mudstones, flat-pebble conglomerates, microbial mounds, and bivalve and crinoid packstones (e.g., Pruss et al., 2005b, 2006). The presence of crinoids indicates deposition under normal marine conditions, and sedimentary features, including packstone

* Authors contributed equally to this study.

 0883-1351/09/0024-0131/$3.00

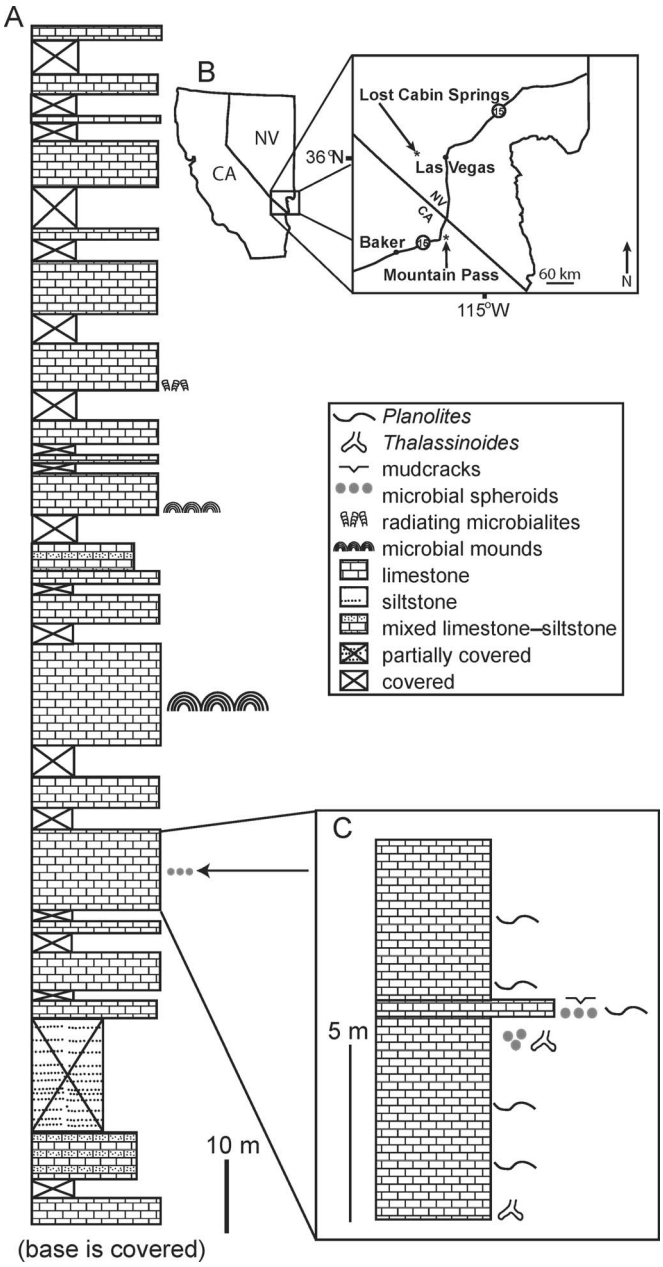

FIGURE 1—Location and stratigraphy of the Lower Triassic Virgin Limestone Member, Moenkopi Formation, Nevada. A) General stratigraphic column of the Virgin Limestone Member measured at the Lost Cabin Springs locality (modified from Pruss and Bottjer, 2004a, 2004b; Pruss et al., 2005b). B) Location map showing Lost Cabin Springs (36°04′56″N, 115°39′11″W) and Mountain Pass localities (35°28′28″N, 115°32′32″W). C) Detailed stratigraphy of carbonate beds above and below the spheroid-bearing strata; flooding surface occurs directly above the unit containing mudcracks and abundant microbial spheroids.

beds and mudcracks, indicate that deposition occurred above storm-wave base, at times in a peritidal environment.

Spheroids occur ~50 m above the exposed base of the section (Fig. 1A), within a ~10-m-thick carbonate interval (Fig. 1C) that crops out as a ledge. Spheroids are preserved on a mud-cracked surface as well as in a few lenses (Fig. 2). The base of the carbonate ledge in which spheroids are found contains well-preserved *Thalassinoides* burrows that are commonly infilled with skeletal debris (crinoids and mollusks). About 6.5 m of bioturbated carbonate (ichnofabric index, ii, of 4–5; *sensu* Droser and Bottjer, 1986) with abundant *Planolites* overlies the *Thalassinoides* bed. Near the top of this unit, a few spheroids are preserved in 5–10-cm-thick lenses (Fig. 2C) near *Thalassinoides* burrows. Overlying the bioturbated unit, a 0.50-m-thick fossiliferous packstone is exposed and preserves abundant spheroids (Fig. 2A–B). The upper 20 cm of this bed has the best-developed spheroids and contains distinct *Planolites* burrows. In this bed, the spheroids are preserved in a few thin lenses (Fig. 2D) and are also preserved on the top of a bedding plane exposed on a large talus block of this 0.5-m-thick carbonate unit (Fig. 2A–B). The talus block had only moved a few meters and could be matched to its original location on the outcrop. The bedding plane on which the spheroids are preserved also contains mudcracks (Fig. 2B). The mud-cracked surface of the talus block was matched to the corresponding horizon on the outcrop, where the surface was overlain by 4.5 m of thinly bedded limestones with ichnofabric indices (ii) alternating throughout the unit between 1–5.

Carbonates of the Virgin Limestone Member at the Mountain Pass locality in southeastern California (~150 km south of Las Vegas; Fig. 1) are lithologically similar to those exposed at Lost Cabin Springs. Carbonate facies at this site are predominantly thinly bedded carbonate mudstones and 0.5–1-m-thick graded storm beds containing abundant *Thalassinoides* burrows (Pruss and Bottjer, 2004a; Pruss et al., 2005a). At this locality, the Virgin Limestone Member was also deposited in a mixed carbonate-clastic shelf environment above storm-wave base. Spheroids are not well preserved at Mountain Pass and occur in only a few 10–50-cm-thick beds within the basal 20 m of the section.

METHODS

All samples described below were collected at Lost Cabin Springs, where spheroids were preserved both on a bedding plane and within a few 5–10-cm-thick lenses. Spheroids at the Mountain Pass locality were more poorly preserved and were largely recrystallized. Diameters of a subset of spheroids at Lost Cabin Springs were measured within a 10 × 10 cm quadrant from a large population of spheroids (>100) that were preserved on an exposed bedding plane containing mudcracks (Fig. 2A–B). The subset of spheroids was measured in the field to ascertain the average size of spheroids within a fixed area. Because the best-preserved spheroids were located in the center of a bedding plane, sampling of these specimens was primarily limited to talus pieces and a few *in situ* samples. Several spheroids were observed in outcrop, but only 11 specimens could be extracted for further petrographic analysis. Limestone samples containing spheroids were then cut perpendicular as well as parallel to bedding, and thin sections of the spheroids were prepared for transmitted light microscopy.

RESULTS

Field Observations

At both localities, spheroids are preserved in packstones containing common crinoid ossicles and rare molluscan shells. The confinement of spheroids to discrete pockets within individual beds suggests that the spheroids were transported and deposited as lenses or in depressions during sedimentation events (Fig. 2). The lack of deformation of individual spheroids further suggests these were at least semi-lithified prior to transport or reworking; however, thin sections reveal that stylolitization of individual spheroids did occur after deposition (Fig. 3). At the Lost Cabin Springs locality, a large population of spheroids was preserved on a mud-cracked bedding plane exposed over ~10 m² (Fig. 2A–B). This mud-cracked surface represents exposure at the top of a parasequence within ~10 m of carbonates (Fig. 1). Here, the spheroids appear to have been transported into an intertidal environment, where they likely became trapped in shallow depressions between mudcracks (Fig. 2B). Atop the mud-cracked surface, a flooding surface is preserved, where deposition of thinly bedded limestones is interpreted to reflect a deepening event.

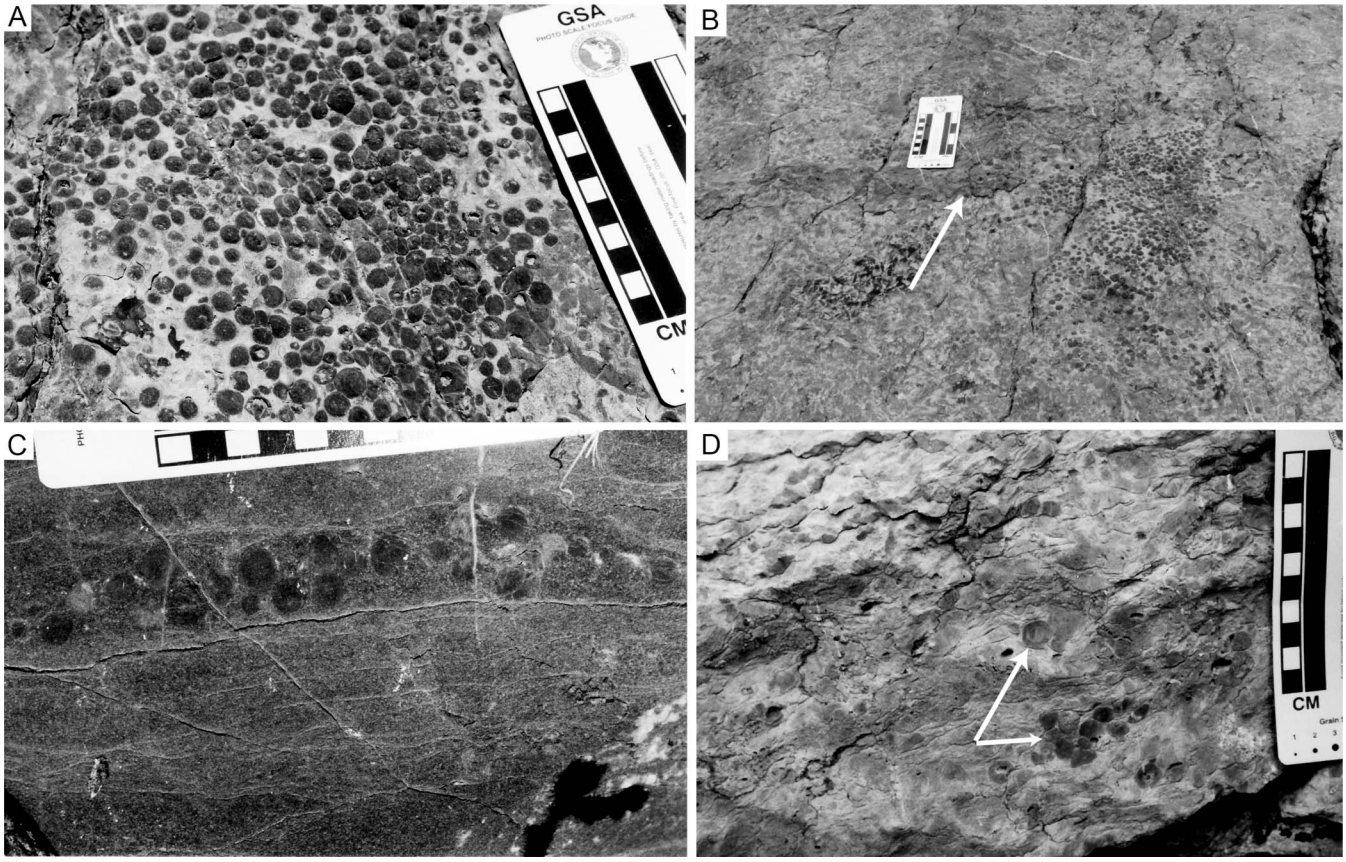

FIGURE 2—Field photographs of microbial spheroids and associated carbonate facies. A) Abundant spheroids preserved on a mud-cracked and burrowed bedding plane. B) Overview of mud-cracked (see arrow) bedding plane. C) Spheroids occurring in a lens just below bedding plane surface. D) Spheroids (arrows) exposed in cross section at Lost Cabin Springs.

The diameter of individual spheroids ranges from 3 to 12 mm, with a mean of 5.8 mm and a median of 5 mm for a subset of 32 measured spheroids. In outcrop, the spheroids are darker gray in color than the surrounding limestone matrix (Fig. 2). Some broken specimens appear recrystallized near their center.

Petrographic Observations

All collected spheroids were examined in thin section (Figs. 3–4). The spheroids range in diameter from 3 to 12 mm. In thin-section, their internal fabrics consist of aggregated micritic clots, equant calcite, and traces of microbial filaments. They are petrographically distinct from the surrounding matrix, which is rich in crinoid and molluscan skeletal grains (Fig. 4D). Spheroids do not incorporate skeletal grains or non-skeletal clasts. The boundaries between spheroids and sedimentary matrix are typically sharp and distinct in thin section (Fig. 3B), although stylolitization of individual spheroids can obfuscate boundaries (Fig. 3A). The spheroids often consist of a framework of aggregated micrite clots near their centers (Figs. 4A, E–F). Individual clots become less distinct near the margins of the spheroids, where the texture consists of micrite with common, thin ghosts of filaments 10–20 μm in diameter (Fig. 4B–D). Based upon these features, it is likely that these spheroids are constructional grains rather than diagenetic concretions. The most common microfabric preserved in the spheroids is a clotted texture consisting of irregularly clustered micrite clots up to 100 μm across (Fig. 4E). Closely spaced clusters of micrite clots are often bridged by microspar cement (Fig. 4E–F). Micritic clots and micrite surrounding individual ghosts of filaments, which we interpret as of probable cyanobacterial origin, constitute the first generation of carbonate precipitation. Brownish microspar cement that occurs between individual micrite clots represents a second generation of carbonate precipitation. Sparry calcite represents a third generation of precipitation and occludes void space within the spheroids. Sparry calcite is most abundant at the center of individual spheroids and decreases in abundance radially. In some cases, sparry calcite may reflect diagenetic replacement of clotted micrite near the center of individual spheroids (Fig. 4B). The spheroids do not exhibit any evidence of layering or trapping of carbonate clasts. Moreover, none of the examined specimens incorporate any preserved skeletal grain or lithoclast as a nucleus.

DISCUSSION

These Lower Triassic spheroids are similar to oncoids in that they likely formed from microbial processes (e.g., Peryt, 1981; Flügel, 2004), but they are not laminated. The absence of preserved layering in the spheroids and the lack of evidence for compaction or deformation before burial indicate rapid accretion and lithification of the entire spheroid. Together, the preservation of individual replaced filaments, micritic clots bridged by microspar cements that were likely penecontemporaneous with spheroid formation, and the lack of evidence for compaction indicate that these grains lithified early and formed via precipitation of calcium carbonate rather than gradual accretion of micritic sediment by a microbial community. The round shape of the microbial spheroids strongly suggests they were unattached and mobile during formation, but it is difficult to determine if this played a role in the radial distribution of microbial fabrics preserved within the spheroids.

Lower Triassic carbonate strata contain abundant non-skeletal facies (e.g., Schubert and Bottjer, 1992; Sano and Nakashima, 1997; Kershaw

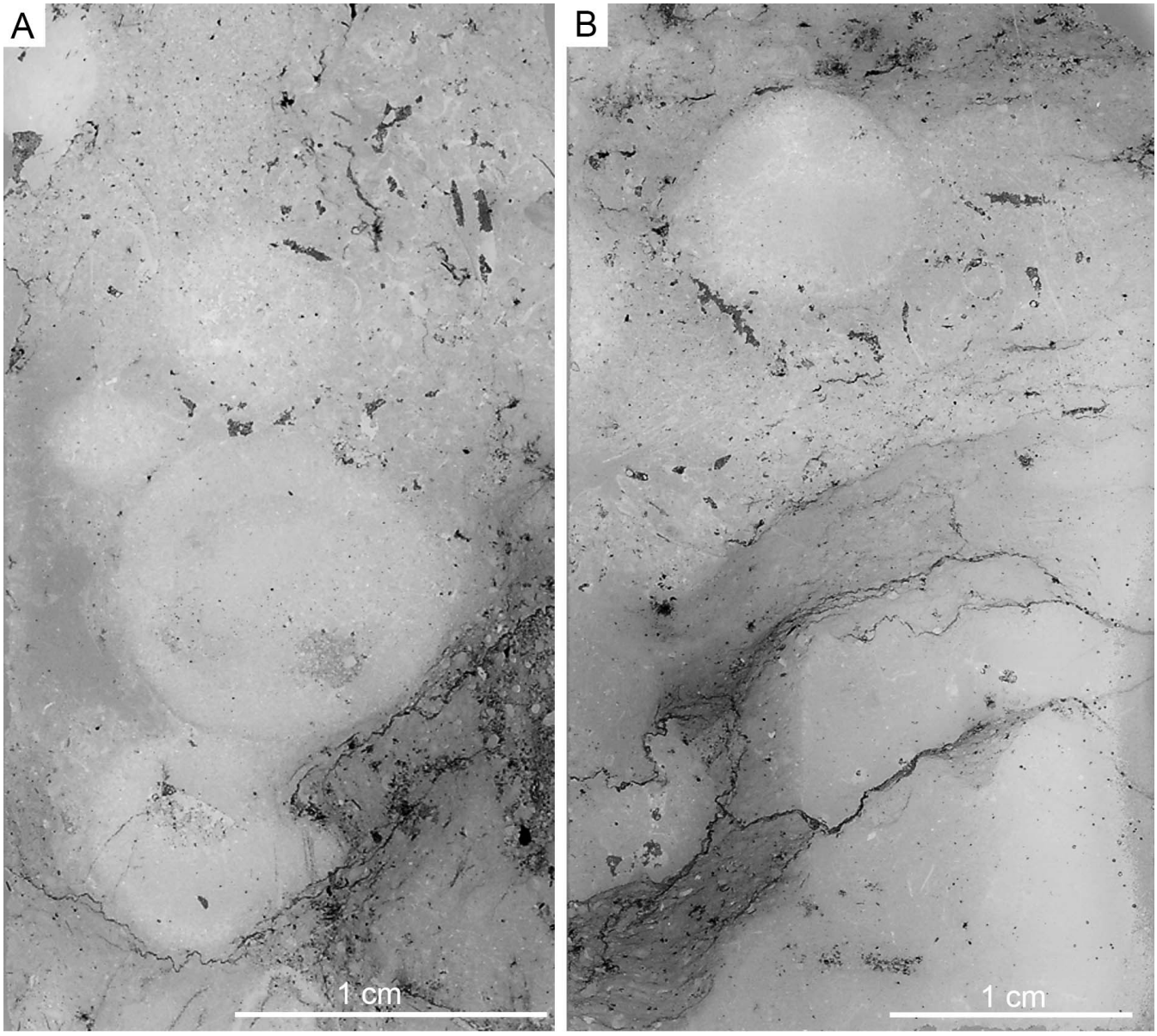

FIGURE 3—Thin sections containing microbial spheroids. A) Four spheroids preserved near each other; note stylolite that dissolves edge of microbial spheroid (bottom); Figure 4D shows a close-up view of this contact. B) Cross-sectional shape of microbial spheroid is strongly circular, suggesting these specimens were spherical when formed.

et al., 1999; Lehrmann, 1999; Lehrmann et al., 2001, 2003; Kershaw et al., 2002; Hips and Hass, 2006; Pruss et al., 2006; Payne et al., 2006). Microbial oncoids, in particular, have been reported from Lower Triassic strata in Iran, Oman, and Japan (Sano and Nakashima, 1997; Baud et al., 2007), as have microspheres from Lower Triassic boundary sections (Wignall and Hallam, 1996; A. Baud, personal communication, 2006). The spheroids described here are much larger than reported oncoids and microspheres, so it is difficult to determine if all of these features share a common mode of formation. Microspheres reported from South China are recrystallized, but may have a microbial origin (Wignall and Hallam, 1996). Based on field and thin-section observations, the spheroids in the Moenkopi Formation are best interpreted as unattached microbial carbonate precipitates. The absence of any preserved laminae in the spheroids, despite high quality textural preservation, indicates that the spheroids precipitated and lithified rapidly, or at least continuously. Thrombolitic carbonate microbialites are a common feature in the Virgin Limestone Member and formed in various paleoenvironments. Many of the microbialites nucleated on cohesive beds or carbonate clasts (Pruss and Bottjer, 2004b; Pruss et al., 2005a, 2005b). In the absence of a firmground for colonization, or perhaps in the presence of a high-energy environment, unattached microbial communities may have served as sites of carbonate precipitation resulting in the precipitation of spheroidal grains.

Microbial spheroids are one component of a nonskeletal Early Triassic carbonate factory within the Virgin Limestone Member (Pruss et al., 2005b). They also represent another manifestation of nonskeletal carbonate depositional modes that were abundant during the Early Triassic, reflecting the long-term impact of the end-Permian mass extinction event on the sedimentary rock record.

ACKNOWLEDGMENTS

SP would like to thank D. Bottjer and F. Corsetti for helpful conversations. P. Wignall, S. Kershaw, and anonymous reviewers provided valuable feedback on this manuscript.

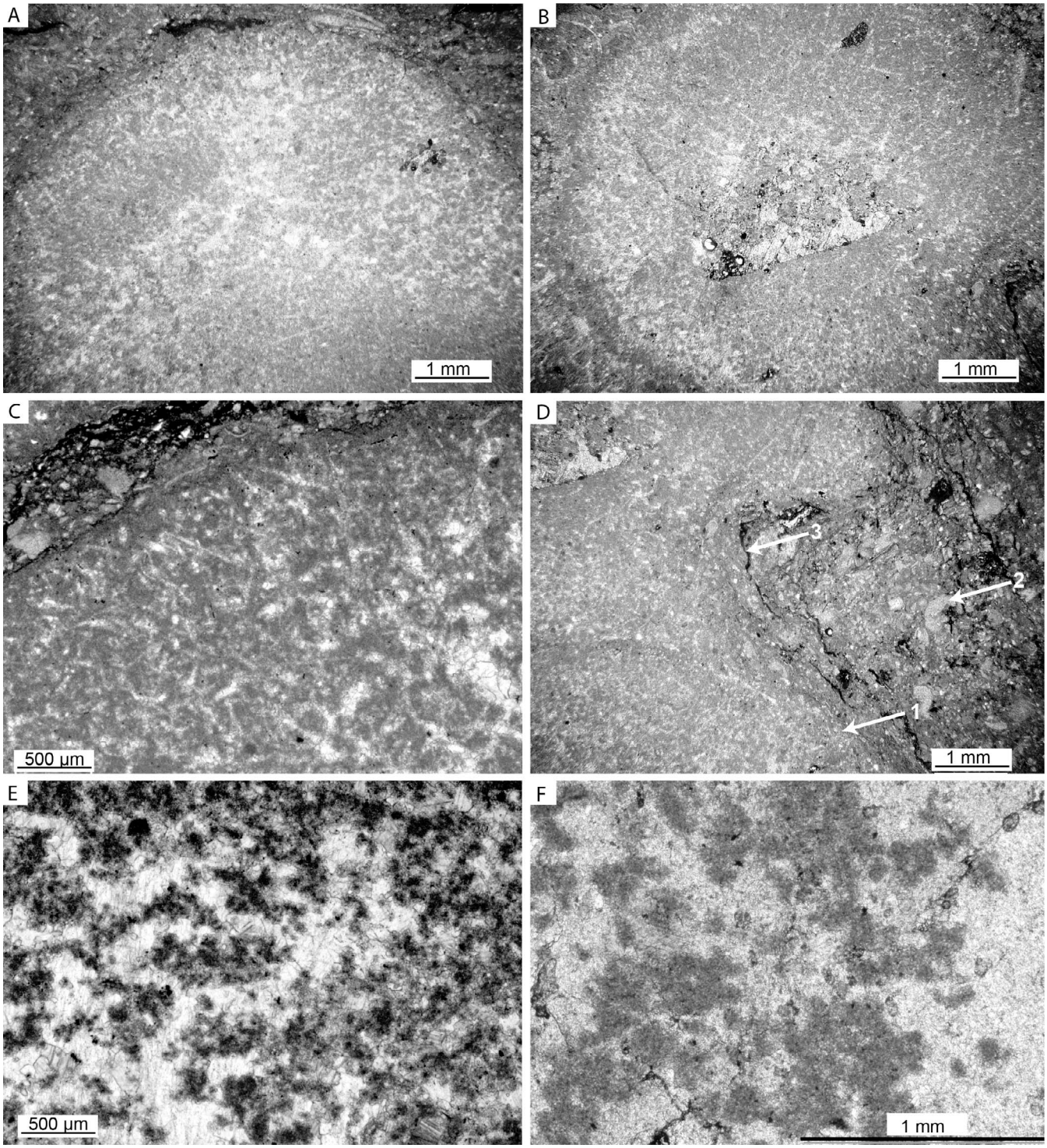

FIGURE 4—Photomicrographs of spheroids in thin section. A) Cross section of a spheroid illustrating diffuse internal microbial fabric that contrasts with surrounding matrix. B) Complete spheroid showing filamentous fabric near the edges and recrystallized center. C) Detail of filamentous fabric commonly preserved near the edges of the spheroids. D) Close up of spheroids pictured in Figure 3A; arrow 1 = margin of spheroid; arrow 2 = echinoderm plate present in fossil debris of which matrix is composed; arrow 3 = stylolite. E) Detail of micrite clots near the center of a spheroid, illustrating microcrystalline cement connecting many of the micrite clots. F) Magnified view of micrite clots.

REFERENCES

Bambach, R.K., Knoll, A.H., and Sepkoski, J.J., 2002, Anatomical and ecological constraints on Phanerozoic animal diversity in the marine realm: Proceedings of the National Academy of Sciences, USA, v. 99, p. 6854–6859.

Baud, A., Cirilli, S., and Marcoux, J., 1997, Biotic response to mass extinction: The lowermost Triassic microbialites: Facies, v. 36, p. 238–242.

Baud, A., Richoz, S., and Marcoux, J., 2005, Calcimicrobial cap rocks from the basal Triassic units: Western Taurus occurrences (SW Turkey): Comptes Rendus Palevol, v. 4, p. 501–514.

Baud, A., Richoz, S., and Pruss, S.B., 2007, Lower Triassic anachronistic carbonate facies in space and time: Global and Planetary Change, v. 55, p. 81–89.

Droser, M.L., and Bottjer, D.J., 1986, A semiquantitative field classification of ichnofabric: Journal of Sedimentary Petrology, v. 56, p. 558–559.

Ezaki, Y., Liu, J.B., and Adachi, N., 2003, Earliest Triassic microbialite micro- to megastructures in the Huaying area of Sichuan Province, South China: Implications for the nature of oceanic conditions after the end-Permian extinction: PALAIOS, v. 18, p. 388–402.

Flügel, E., 2004, Microfacies of carbonate rocks: Springer, Berlin, 976 p.

Groves, J.R., and Calner, M., 2004, Lower Triassic oolites in Tethys: A sedimentologic response to the end-Permian mass extinction: Geological Society of America Annual Meeting, Abstracts with Program, v. 36, p. 336.

Hips, K., and Hass, J., 2006, Calcimicrobial stromatolites at the Permian–Triassic boundary in a western Tethyan section, Bükk Mountains, Hungary: Sedimentary Geology, v. 185, p. 239–253.

Kershaw, S., Zhang, T.S., and Lan, G.Z., 1999, A ?microbialite carbonate crust at the Permian–Triassic boundary in South China, and its palaeoenvironmental significance: Palaeogeography, Palaeoclimatology, Palaeoecology, v. 146, p. 1–18.

Kershaw, S., Guo, L., Swift, A., and Fan, J.S., 2002, Microbialites in the Permian–Triassic boundary interval in central China: Structure, age and distribution: Facies, v. 47, p. 83–89.

Lehrmann, D.J., 1999, Early Triassic calcimicrobial mounds and biostromes of the Nanpanjiang basin, south China: Geology, v. 27, p. 359–362.

Lehrmann, D.J., Wan, Y., Wei, J.Y., Yu, Y.Y., and Xiao, J.F., 2001, Lower Triassic peritidal cyclic limestone: An example of anachronistic carbonate facies from the Great Bank of Guizhou, Nanpanjiang Basin, Guizhou Province, South China: Palaeogeography, Palaeoclimatology, Palaeoecology, v. 173, p. 103–123.

Lehrmann, D.J., Payne, J.L., Felix, S.V., Dillett, P.M., Wang, H., Yu, Y.Y., and Wei, J.Y., 2003, Permian–Triassic boundary sections from shallow-marine carbonate platforms of the Nanpanjiang Basin, south China: Implications for oceanic conditions associated with the end-Permian extinction and its aftermath: PALAIOS, v. 18, p. 138–152.

McGhee, G.R., Sheehan, P.M., Bottjer, D.J., and Droser, M.L., 2004, Ecological ranking of Phanerozoic biodiversity crises: Ecological and taxonomic severities are decoupled: Palaeogeography, Palaeoclimatology, Palaeoecology, v. 211, p. 289–297.

Payne, J.L., Lehrmann, D.J., Wei, J., and Knoll, A.H., 2006, The pattern and timing of biotic recovery from the end-Permian extinction on the Great Bank of Guizhou, Guizhou Province, south China: PALAIOS, v. 21, p. 63–85.

Peryt, T.M., 1981, Phanerozoic oncoids: An overview: Facies, v. 4, p. 197–214.

Poborski, S.J., 1953, The Virgin Formation of the Saint George, Utah, area: Plateau, v. 25, p. 69–79.

Pruss, S., and Bottjer, D.J., 2004a, Early Triassic trace fossils of the western United States and their implications for prolonged environmental stress from the end-Permian mass extinction: PALAIOS, v. 19, p. 551–564.

Pruss, S.B., and Bottjer, D.J., 2004b, Late Early Triassic microbial reefs of the western United States: A description and model for their deposition in the aftermath of the end-Permian mass extinction: Palaeogeography, Palaeoclimatology, Palaeoecology, v. 211, p. 127–137.

Pruss, S.B., Corsetti, F.A., and Bottjer, D.J., 2005a, Environmental trends of Early Triassic biofabrics: Implications for understanding the aftermath of the end-Permian mass extinction, *in* Morrow, J.D., Over, D.J., and Wignall, P.B., eds., Understanding Late Devonian and Permian–Triassic Biotic and Climatic Events: Toward an Integrated Approach: Elsevier, Amsterdam, p. 313–332.

Pruss, S.B., Corsetti, F.A., and Bottjer, D.J., 2005b, The unusual sedimentary rock record of the Early Triassic: A case study from the southwestern United States: Palaeogeography, Palaeoclimatology, Palaeoecology, v. 222, p. 33–52.

Pruss, S.B., Corsetti, F.A., Bottjer, D.J., and Baud, A., 2006, A global marine sedimentary response to the end-Permian mass extinction: Examples from southern Turkey and the western United States: Earth-Science Reviews, v. 78, p. 193–206.

Raup, D.M., 1979, Size of the Permo–Triassic bottleneck and its evolutionary implications: Science, v. 206, p. 217–218.

Raup, D.M., and Sepkoski, J.J., 1982, Mass extinctions in the marine fossil record: Science, v. 215, p. 1501–1503.

Sano, H., and Nakashima, K., 1997, Lowermost Triassic (Griesbachian) microbial bindstone-cementstone facies, southwest Japan: Facies, v. 36, p. 1–24.

Schubert, J.K., and Bottjer, D.J., 1992, Early Triassic stromatolites as post mass extinction disaster forms: Geology, v. 20, p. 883–886.

Shorb, W.M., 1983, Stratigraphy, facies analysis and depositional environments of the Moenkopi Formation (Lower Triassic), Washington County, Utah, and Clark and Lincoln Counties, Nevada: Unpublished M.Sc. thesis, Duke University, Durham, North Carolina, 205 p.

Wignall, P.B., and Hallam, A., 1996, Facies change and the end-Permian mass extinction in S.E. Sichuan, China: PALAIOS, v. 11, p. 587–596.

Wignall, P.B., and Twitchett, R.J., 1999, Unusual intraclastic limestones in Lower Triassic carbonates and their bearing on the aftermath of the end-Permian mass extinction: Sedimentology, v. 46, p. 303–316.

Woods, A.D., Bottjer, D.J., Mutti, M., and Morrison, J., 1999, Lower Triassic large sea-floor carbonate cements: Their origin and a mechanism for the prolonged biotic recovery from the end-Permian mass extinction: Geology, v. 27, p. 645–648.

ACCEPTED AUGUST 9, 2008